Construction and Building Materials 408 (2023) 133583

Contents lists available at ScienceDirect

Construction and Building Materials

journal homepage: www.elsevier.com/locate/conbuildmat

Review

Non-destructive techniques (NDT) and statistical analysis for the characterization of bricks made with added glass

L. Crespo-López [a,*], D. Benavente [b], S. Morales-Ruano [a,c], M. Vázquez-Vílchez [d], G. Cultrone [a]

[a] Department of Mineralogy and Petrology, Faculty of Sciences, University of Granada, Avda. Fuentenueva s/n, 18002 Granada, Spain
[b] Department of Environmental and Earth Sciences, University of Alicante, 03690 San Vicente del Raspeig, Spain
[c] Andalusian Institute of Earth Sciences, (IACT), University of Granada-CSIC, Avda. de las Palmeras, 4, 18100 Armilla, Granada, Spain
[d] Department of Didactics of Experimental Sciences, Faculty of Education Sciences, University of Granada, 18071 Granada, Spain

ARTICLE INFO

Keywords:
Physical-mechanical properties
Handmade bricks
ANOVA
Characterisation
Building materials
Environmental savings

ABSTRACT

The aim of this paper was to assess how adding crushed household glass to the clay mix affects the properties of handmade bricks. To this end, non-destructive techniques (NDT) were used to characterize solid bricks made with two mineralogically different clays with or without the glass additive. One of the clays (Jun) was rich in carbonates, while the other (Guadix) was richer in silicates and had no carbonates. The use of NDT combined with statistical analysis of the initial hypotheses proved to be a very useful method for evaluating whether these handmade bricks are suitable and efficient for use in heritage restoration and the construction industry in general. A second objective was to assess whether the firing temperature influenced the aesthetic (tested using videomicroscopy, colour measurement and radiography) and physical–mechanical (Leeb hardness test, ultrasonic pulse velocity and compressive strength) properties of the bricks. The addition of glass increased the vitrification and compressive strength of the bricks. The colour varied according to the raw materials used and the firing temperature. Radiography proved to be a very useful tool for observing the heterogeneous distribution of the density. In terms of physical–mechanical properties, the bricks from Jun performed better than those from Guadix, as confirmed by ANOVA analysis. However, the more pronounced variation in the colour of the bricks from Jun fired at 1100 °C made with added household glass could make them less suitable for heritage restoration work, where matching colours are a crucial factor.

1. Introduction

Handmade bricks are used throughout the world, often in combination with stone masonry and timber roofs or floors. This is because bricks are easy to produce, easy to shape and in most cases are lighter than stone, forming fire-resistant, durable walls. Bricks are made of clay, a natural, non-renewable resource. One option to help reduce the continuous depletion of this resource would be to use waste products that would otherwise accumulate in landfills as additives in the brick production process, so reducing the amount of clay required [1]. This in turn would reduce the need for clay extraction, a process that causes environmental disturbances, through soil erosion, and produces pollutants such as particulate matter. It also results in the emission of gases such as carbon monoxide, carbon dioxide, nitrogen oxides and sulphur oxides [2]. This is why some governments, such as the Chinese, are discouraging the use of clay bricks and promoting eco-friendly construction materials after an annual loss of 66.7 million square meters of fertile land due to the extraction of clay for brick production [3]. In research into these materials, it has been observed for example that bricks made exclusively with water treatment sludge or with sludge and other residues proved highly weather-resistant [3]. Various studies have been conducted recently to investigate the reuse of wastes in the production of building materials in general [4–5] and of bricks in particular [6–16]. Promising, yet contrasting, results have been obtained in terms of the porosity of fired samples, as in the case of Fe-rich metallurgical wastes [12]. The use of certain waste products as additives in brick manufacture can improve the properties of the bricks (porosity, strength, durability, etc.) and promote sustainability through recycling [11]. This study goes beyond the interesting, descriptive analysis typically provided by these previous studies, and uses statistical techniques such as analysis of variance or factorial analysis to assess the influence of using additives on the physical properties of the bricks. In this case, it

* Corresponding author.
E-mail address: lcrespo@ugr.es (L. Crespo-López).

https://doi.org/10.1016/j.conbuildmat.2023.133583
Received 11 December 2022; Received in revised form 13 September 2023; Accepted 27 September 2023

was decided to investigate the use of household glass as an additive in brick production to enable, on the one hand, the reuse of domestic glass waste, so promoting the circular economy, and on the other to reduce the amount of clay required to produce the bricks. The reuse of waste glass in this way would also produce energy savings and environmental benefits by reducing the need for landfill. The final aim was to produce highly efficient handmade bricks for use in heritage restoration and new buildings, of higher quality than those currently available.

The petrophysical properties of handmade bricks are very important for the structural behaviour of both modern and historic buildings in that they are the main factor influencing the compressive strength of the masonry [14]. Recent studies have proposed new approaches in the characterization of historic building materials [17–19]. When carrying out an exhaustive characterization of the materials used in a building, a series of precautions must be taken, so as to avoid compromising the stability of the structure. Whenever possible, non-destructive techniques (NDT) should be used. Researchers analysing the petrophysical characteristics of bricks have used NDT to explore their physical properties and interpret them on the basis of their petrographic characteristics, assessing the pores, fissures, anisotropies, hardness, chemistry and mineralogy of the fired samples [20,21]. NDT are easier to use in bricks than in other materials such as stone. This is because bricks are almost homogeneous materials. They have no internal discontinuities and are fairly isotropic, which makes it much easier to interpret the results obtained and to apply the basic principles of elementary physics, which are based on assumptions regarding the behaviour of homogeneous, isotropic materials with no discontinuities [22]. For these reasons, in this paper, NDT were combined with statistical analysis to create a useful method for the safe assessment of the state of both historic buildings and modern constructions. Some of these NDT, such as ultrasonic pulse velocity (UPV) or the Leeb hardness (LH) test, can be applied in situ, an important consideration in heritage restoration. This methodology enabled the accurate characterization of the components of the building materials and provided information about their physical and mechanical properties.

The main objective of this paper was to use non-destructive and statistical techniques to determine whether handmade bricks were suitable and efficient for use in building restoration and in the construction industry in general. An attempt was also made to assess whether the addition of crushed household glass improved the properties of the bricks, and whether the firing temperature affected their aesthetic and physical–mechanical properties.

2. Materials and methods

2.1. Production of bricks

The bricks used in this research were made of clay from two localities, Guadix (G) and Jun (J) (Granada, Spain), about 50 km apart. Both these clays are post-orogenic, continental sediments deposited in the intermontane basins of Guadix-Baza and Granada. The clay from Guadix was deposited in the middle-late Pleistocene during the last stages of the infilling of the basin [23–25], above all in small lakes and swamps that developed temporarily on the banks of braided rivers that drained from the nearby Sierra Nevada mountains [23]. The clay from Jun was deposited during the late Turolian in a lacustrine environment with nearby fan deltas that drained carbonate sediments eroded from Sierra Arana [26].

In order to test the possible use of glass as an additive, 20 wt% crushed household glass was added to clay mixes from Guadix and Jun. The bricks were fired and then compared with other bricks made without glass, which served as the control group. Both brick types, with or without waste glass, were handmade. The decision as to how much glass to add (20 wt%) was based on recent investigations with promising results [27–29]. The clay (from Guadix and Jun) was sieved, so as to remove fragments of over 1.5 mm in size prior to mixing with glass (when present) and water. The mixture was then kneaded until sufficient plasticity was achieved. 308 ml/kg and 333 ml/kg of kneading water were needed for bricks with or without glass, respectively. The clayey paste was then placed in moistened wooden moulds of 15 × 20 × 4 cm. After one hour, the moulds were removed from the clayey paste and cut into 4 cm edge cubes using a stretched cotton thread (Fig. 1A).

When the bricks were totally dry, they were fired in a Herotec CR-35 electric oven at 800 °C, 950 °C and 1100 °C (Fig. 1B and C). Once the desired temperature was reached, it was kept constant for 3 h. Then the oven was turned off and the samples were left inside to cool until the next day. Slow cooling in this way prevents the development of fissures due to β-to-α quartz transition at 573 °C. Finally, the fired samples were removed from the oven and immersed in water for about 1 h so as to avoid "lime blowing" due to the presence of lime grains [30]. Table 1 shows the acronyms assigned to the 12 types of bricks studied in this paper.

2.2. Methods

The following methodology was used to study the raw materials and the fired bricks. The first step was to characterize the two raw materials and the fired bricks in order to determine their chemical–mineralogical composition. To this end, a Fourier transform infrared spectroscopy using an attenuated total reflectance sample holder (ATR-FTIR) was used and the mineralogical information was obtained by powder X-ray diffraction (PXRD) using a PANalytical X'Pert PRO diffractometer. The working conditions were: CuKα radiation, 45 kV voltage, 40 mA current, 3 to 70° 2θ exploration range, 0.1 2θ s^{-1} goniometer speed. The mineral phases were identified using the PANalytical X'pert Highscore Plus 3.0 software. In order to identify the clay fraction more accurately, the following oriented aggregates were prepared according to the recommendations of Moore and Reynolds [31]: air dried, solvated with ethylene glycol, solvated with dimethyl sulfoxide and heated at 550 °C. The qualitative determination of the compositional vibrations of the raw materials and the household glass was analysed by ATR-FTIR, within a frequency range of 4000–400 cm^{-1} and with a step size of 0.50 cm^{-1}.

Videomicroscopy, radiography and spectrophotometry were used to assess the appearance of the fired bricks. A Leica DVM 2000 digital videomicroscope, using the Leica Application Suite V.3.8.0 for photo acquisition, was used as a preliminary tool to identify textural differences and relevant features on the surface of the samples with a higher magnification than the naked eye. A Konica Minolta CM-700d spectrophotometer was used to quantify the colour of the bricks according to the UNE-EN 15886 standard [32]. Illuminant D65, 10° observer and 8 mm measurement area were used. Nine measurements per sample were performed to determine their lightness (L*) and chromatic values (a* and b*).

Radiography is a useful NDT for detecting possible non-visible defects in the bricks as its shortwave elementary particles can penetrate the bricks without causing any damage. In particular, X-rays were used to detect significant differences in the degree of vitrification of the bricks made with or without glass. X-rays were carried out using a TROPHY radiologic VETOX 11ST with 95 kV and 50 mA working conditions. A Micro Computer with METRON-DVM software was used to process the radiographic images.

Finally, the physical–mechanical properties of the bricks were evaluated using the LH and UPV tests. The uniaxial compression (CS) test, which causes the samples to break and become unusable, was used to confirm the results obtained with LH and UPV. The LH tester PCE-2500N was used for the non-destructive measurement of the surface hardness of bricks using a rebound hammer. The brick cubes were cut in half and 5 linear measurements per brick were made from the left outer edge through the core to the right outer edge. The harder the surface of the material, the higher the rebound speed. UPV is increasingly mentioned in the literature, especially in Europe, due to the possibility of establishing a correlation between CS and UPV [18,19]. UPV measures the

Fig. 1. Photograph of the bricks studied in this work. A) Unfired bricks made from raw materials from Jun and Guadix with and without household glass; B-C) General view of fired bricks with and without household glass.

Table 1
Acronym assigned to each brick according to the raw material used, the addition of 20 wt% household glass and the firing temperature.

Raw materials	Firing temperature (°C)	Additive	
		without glass	with glass
Jun (J) and Guadix (G)	800	J800	Jg800
		G800	Gg800
	950	J950	Jg950
		G950	Gg950
	1100	J1100	Jg1100
		G1100	Gg1100

degree of compactness and was used to determine the elastic-dynamic properties of the bricks, properties that affect their mechanical resistance [33]. Measurements were performed using a Control 58-E4800 ultrasonic pulse velocity tester with transducers of 54 kHz and a circular surface of 27 mm in diameter. A water-based eco-gel was used to enable homogeneous contact between the transducers and the brick surfaces. The measurements were carried out on three samples per brick type. P-wave propagation was measured in m/s according to the ASTM D2845 [34] standard.

The compressive strength (Rc) was measured using a Matest E181 hydraulic press with double frame 25 kN/300 kN according to the UNE-EN 772-1 [35] standard. Rc was calculated in MPa on three samples of each brick according to the following Eq. 1:

$Rc = \frac{F}{A}$ (1)

Where F is the breaking load (in N) and A is the cross-sectional area in m^2.

The analysis of variance technique (ANOVA) is a statistical test used to compare the means of two or more groups of variables or factors, such as the firing temperature (800 °C, 950 °C and 1100 °C) and the type of raw material used. It can also be used to assess how adding the glass affects the samples. In this analysis, both the effect of each factor on the various parameters studied and the possible interaction between the variables were analysed. Statistically different groups were identified using Tukey's and Duncan's tests ($P < 5$ %). In addition, the experiment and the procedure were checked to ensure that there were no significant errors that would invalidate the study.

3. Results and discussion

3.1. Raw materials

3.1.1. ATR-FTIR

The analysis carried out on the clays from Guadix and Jun and the household glass showed that the bands related to the asymmetric stretching of the Si-O of quartz or free silica (SiO_4) in the region between ~900 and ~1050 cm^{-1} and between ~400 and ~500 cm^{-1} [36–38] are well defined in all the samples. The peak at 1046 cm^{-1} corresponded to the intense Si–O and Si–O–Al stretching frequencies, characteristic of the aluminium silicates [39–40] present in the clayey materials. Peaks were also detected in the region near 475 cm^{-1}, which could correspond to the typical peak of the Fe-O bond of hematite [41]. Another peak appeared near 795 cm^{-1}, which could be attributed to maghemite [42], a polymorphic form of Fe_2O_3 called γ-Fe_2O_3 with an inverse spinel structure, which differentiates it from α-Fe_2O_3 (hematite), which has a corundum structure.

The shoulders observed between 3000 cm^{-1} and 3400 cm^{-1} correspond to the moisture [43] present in the clayey samples (Fig. 2, green and blue lines), while the bands located at ~3600 cm^{-1} (v_1, symmetric stretching) and ~3700 cm^{-1} (v_3, anti-symmetric stretching [44]) correspond to the vibration of the molecules in the O-H group and in Al–OH, which are probably associated with the presence of phyllosilicates [45]. Illite/muscovite may be characterized by OH-stretching around 3620 cm^{-1} [40,46]. The peaks at ~800 and ~750 cm^{-1} confirm the presence of a Si-O-Al stretching frequency where Al is in tetrahedral coordination and support the possible presence of illite or muscovite [45]. The absorption band at 3694–3620 cm^{-1} indicates the stretching vibrations of –OH groups from the kaolinite network [47].

The two clayey samples can be differentiated by the fact that in the raw material from Jun (Fig. 1, green line), the presence of carbonates is corroborated by the appearance of characteristic CO_3^- group (v_2) (~874 cm^{-1}) and CO_3^- group (v_3) (~1430 and ~1460 cm^{-1}) vibrations [48–51].

When characterizing the household glass, the shoulder observed between 800 and 1200 cm^{-1} was taken into account (Fig. 2, orange line). This range houses the Si-O-Ca bonds (980 and 905 cm^1) containing non-bridging oxygen, the O-Si-O bonds (819 cm^{-1}) and symmetric

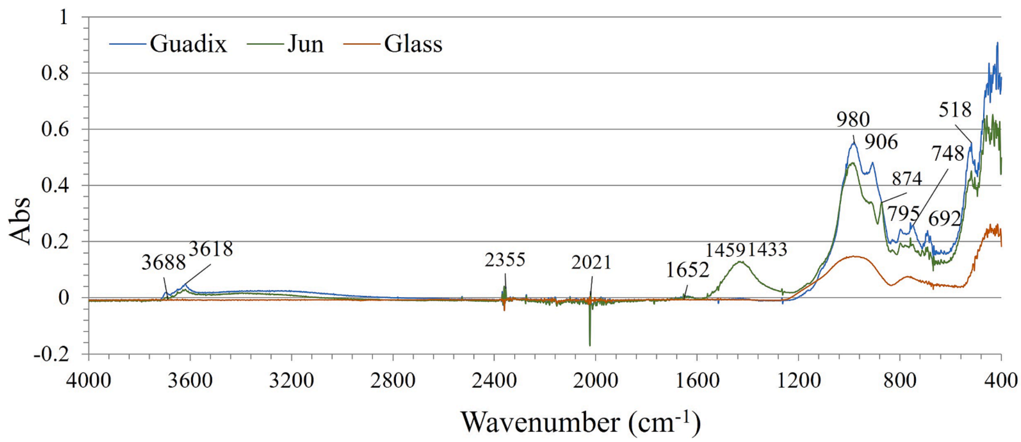

Fig. 2. Infrared absorption spectroscopy carried out on the raw materials from Guadix and Jun and on the household glass.

stretching of the Si-O-Si bonds (1090, 503 and 464 cm^{-1}) [52,53]. MacDonald et al. [54] determined that the presence of alkali ions, such as sodium, adds new vibrational modes, Si-O-[alkali] bending and stretching. These break up the original network, altering the modes associated only with the silica network. The characteristic ranges of these modes (Si-O-[alkali] stretching) are in line with those observed by previous authors [55,56].

3.1.2. PXRD

PXRD analysis of the clays from Jun and Guadix has highlighted the presence in both samples of quartz, k-feldspars and phyllosilicates (illite, paragonite, chlorite and kaolinite) (Fig. 3). The clay from Jun has a

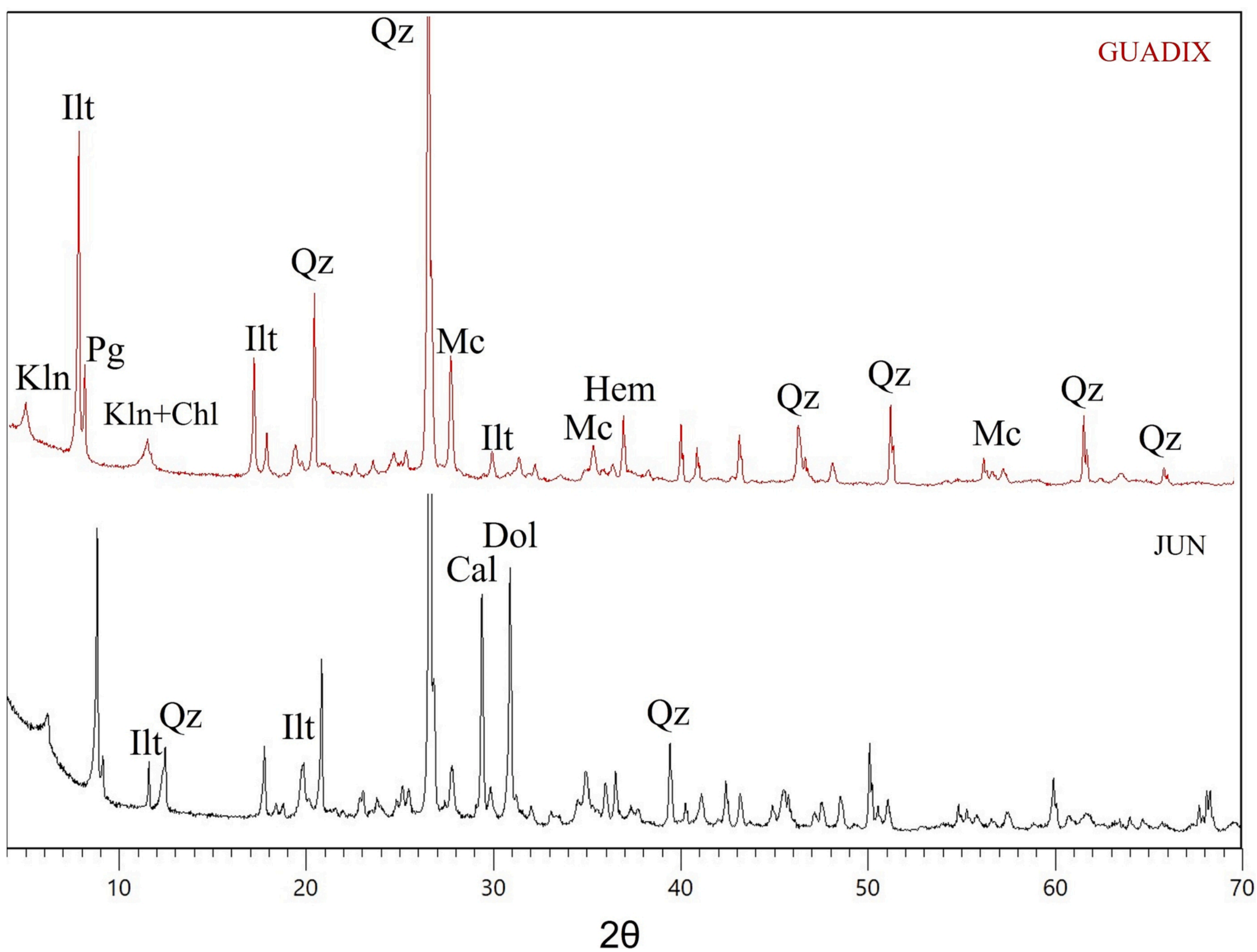

Fig. 3. Mineralogy of the raw materials (Jun and Guadix). Legend according to Warr (2020) [58]: Ilt = illite; Pg = paragonite; Kln = kaolinite; Chl = chlorite; Qz = quartz; Cal = calcite; Dol = dolomite; Mc = microcline; Hem = hematite.

slightly higher concentration of kaolinite, illite and paragonite than the clay from Guadix and the presence of chlorite, a mineral that is commonly masked by smectite (~ 14 Å) and kaolinite (~ 7 Å), has been confirmed by heating the oriented aggregates to 550 °C [57]. Carbonates (calcite and dolomite) and hematite were only detected in the clay from Jun.

3.2. Fired bricks

3.2.1. Mineralogical properties

3.2.1.1. PXRD. PXRD analysis of the bricks from Jun (J) and Guadix (G) fired at 800 °C shows that all the phyllosilicates had disappeared with the exception of dehydroxylated illite, which can still be detected, although the reflection (001) at 10 Å is lower compared to the raw materials, which suggests a lower concentration (Fig. 4). Quartz is the most abundant phase and hematite is beginning to be detected.

In J800, the dolomite has disappeared while calcite is present in smaller concentrations. An increase in the amorphous phase can be detected in samples with added glass (Jg800 and Gg800).

At 950 °C the differences in the samples with or without added glass are more evident than at 800 °C (Fig. 4). In both brick groups, orthoclase is transformed into a higher temperature polymorph phase, sanidine. They also have a higher hematite content probably due to the decomposition of phyllosilicates, which favours Fe recrystallization [59]. In J950, calcite disappeared and new mineral phases, such as gehlenite, wollastonite and diopside, were formed (Fig. 4). According to Rathossi and Pontikes [60], gehlenite is formed by the reaction between illite, calcite and quartz as follows:

Illite	calcite	quartz	gehlenite	sanidine
$KAl_2(Si_3Al)O_{10}(OH)_2+$	$2CaCO_3+$	$SiO_2\rightarrow$	$Ca_2Al_2SiO_7+$	$KAlSi_3O_8 + H_2O + 2CO_2$

In Jg950, other phases such as anorthite appear, while illite disappears. The quartz concentration decreases and high temperature phases (gehlenite, wollastonite, diopside, hematite) are detected in larger amounts than in J950. The addition of glass seems to cause the reactions between the mineral phases to happen earlier. As a result, phases typical of higher firing temperatures begin to appear earlier in the samples with added glass than in the samples made without it [14]. In G950, the illite and quartz content is lower. There is a negligible difference in the mineralogy between the bricks made with added glass (Gg950) and those made without it (G950). Mullite diffraction peaks are more intense in phyllosilicate-rich samples (Guadix) than in carbonate-rich samples (Jun).

At 1100 °C, the changes in the mineralogy produced by the addition of glass are even more distinguishable (Fig. 4). In the bricks made with clay from Jun, the sample fired at 1100 °C without glass (J1000) is mineralogically very similar to the sample fired at 950 °C with glass (Jg950). The two samples have very similar hematite content. The amount of gehlenite decreases in J1100 and disappears completely in Jg1100, as it is involved in the formation of anorthite and wollastonite + diopside [61,62]. In Jg1100, the increase in background noise indicates a larger amount of amorphous phase due to the vitrification of the bricks. This could be due to the fact that, with an increase in firing temperature and vitrification, the silica content of the quartz starts converting into amorphous silica, so adding to the amorphous silica already present in the glass [63]. However, in the samples in which household glass, an amorphous material, is present, the background noise is more noticeable. In the samples made with clay from Guadix fired at 1100 °C, there is little difference in mineralogical terms between the samples made with (Gg1100) or without added glass (G1100) and there is less background noise than in the Jun samples fired at the same temperature.

3.2.2. Assessment of aesthetic properties

3.2.2.1. Videomicroscopy and colour measurement. The colour of the bricks after firing will depend on the composition of the raw materials and the degree of transformation of the bricks during the firing process, which in turn is mainly dependent on the temperature, time and oxidant-redox environment inside the oven [60,64]. The bricks fired at low temperatures (800 °C), with or without added glass, had a reddish appearance (Fig. 5). However, as the firing temperature increased, the difference in colour between the bricks made with clay from Jun and Guadix became more evident. In the bricks fired at 950 °C, a considerable difference in colour can be observed between those made with added glass and those made without it. This may also be due to an apparently higher porosity in the samples fired at higher temperatures. In addition, from 950 °C onwards, "glass bubbles" began to form on the surface of the bricks. These were more evident in the samples made with clay from Guadix (Fig. 5).

The lightness in the bricks from Jun increases in line with the firing temperature (L*, Table 2). The opposite occurs in the Guadix bricks, where a decreasing trend can be observed in average lightness values as the firing temperature increases (L*, Table 2). The average lightness values for the samples with added glass follow a similar pattern to those for the samples without additive, with Jun bricks showing increasing L* values and Guadix bricks showing the opposite tendency. This is probably due to the fact that there are more glass bubbles on the surface of the Guadix bricks, which makes them slightly darker (Fig. 5).

The a* values show a similar trend for both types of bricks. The average values fall as temperature increases, more steeply in the samples with added glass than in those without it, which show a gentler decline. The samples with the lowest b* values are those fired at high temperature with added glass (Gg1100). The samples from Guadix have a more reddish colour than those from Jun with higher a* and b* values. This is due to the crystallisation of iron oxides from the decomposition of phyllosilicates, whereas in the Jun samples, Fe is partly involved in the formation of new Ca-silicates such as gehlenite [65,66].

Fig. 6 shows a volume chart diagram for the L* and a* parameters. The b* parameter was not included in Fig. 6 because the a* values indicate the red/green coordinates (+a indicates red, -a indicates green), the most important parameters in the colour analysis of bricks, which normally have a reddish hue.

Bricks made with both types of clay fired at 800 °C have similar mean L and a* values and a similarly low standard deviation, regardless of whether or not they have added glass. From 950 °C onwards, the samples follow similar trends depending on the composition of the raw material. While the bricks from Jun show greater dispersion, those from Guadix are more homogeneous. This difference in the dispersion values continues at 1100 °C, where the samples from Jun with added glass (Jg1100) have very high (and dispersed) lightness values compared to those from Guadix. This could be related to the fact that the addition of glass gives the Jun bricks fired at 1100 °C a more yellowish colour than the Guadix bricks, which have an intense red tone (Fig. 6). This could

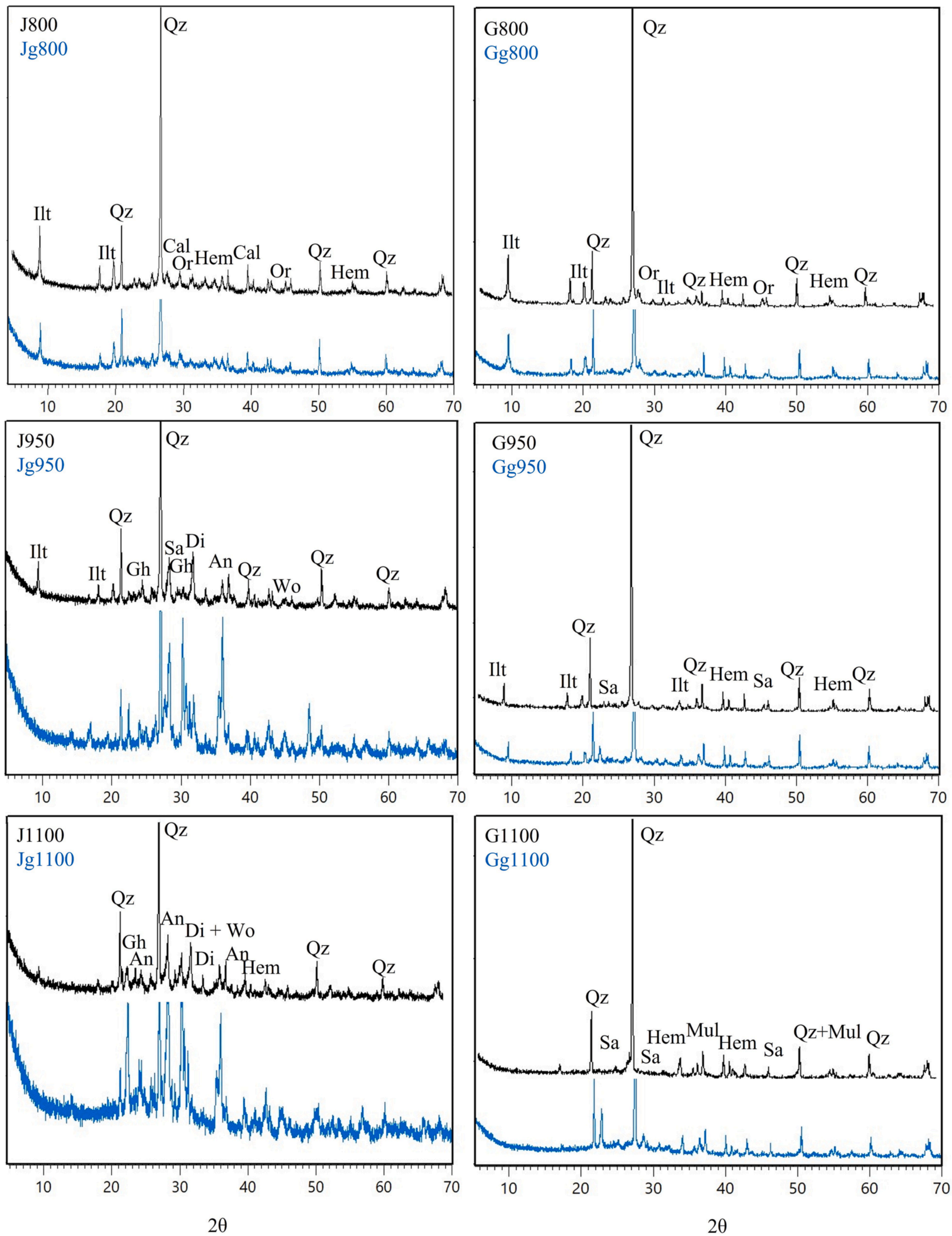

Fig. 4. Mineralogy of the bricks made with clay from Jun (left) and Guadix (right) with and without glass added and fired at different temperatures. Legend (mineral acronyms according to Warr (2020) [58]:): Qz = quartz; Cal = calcite; Ilt = illite; Hem = hematite; Sa = sanidine; Or = orthoclase; An = anorthite; Mul = mullite; Gh = gehlenite; Di = diopside; Wo = wollastonite.

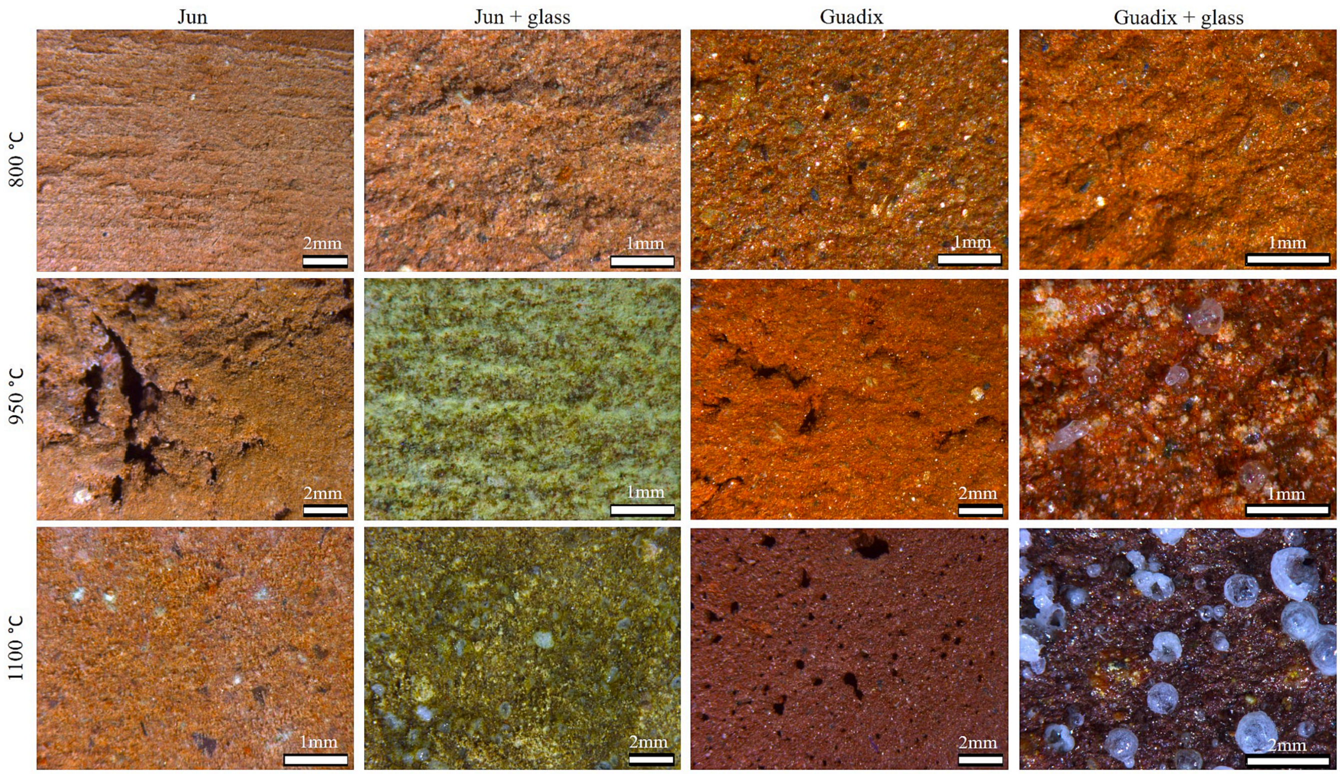

Fig. 5. Macroscopic features of the bricks from Jun (J, first and second columns) and Guadix (G, third and fourth columns) fired at 800, 950 and 1100 °C, with or without added glass (g).

Table 2
Average lightness values (L*), chromatic values (a* and b*) and standard deviation (σ) for handmade bricks made with clay from Jun and Guadix with or without added glass.

		L*		a*		b*	
		$\bar{x}$	Σ	$\bar{x}$	σ	$\bar{x}$	Σ
JUN	J800	58.49	3.11	16.13	0.63	22.90	0.84
	J950	62.96	1.51	15.06	1.22	23.69	2.10
	J1100	62.74	1.43	15.34	1.22	23.02	0.76
	Jg800	59.75	1.05	17.03	0.86	23.83	1.69
	Jg950	73.55	2.50	5.87	0.95	23.35	0.90
	Jg1100	63.01	8.20	6.33	1.03	22.83	1.41
GUADIX	G800	55.01	1.32	21.04	0.95	29.55	1.31
	G950	55.18	2.85	23.70	1.03	31.38	1.16
	G1100	44.12	1.49	20.61	1.66	19.23	2.17
	Gg800	53.26	1.64	21.87	0.93	29.82	1.21
	Gg950	52.00	2.57	22.59	0.97	27.99	2.14
	Gg1100	45.14	1.73	12.17	4.12	10.82	3.35

also explain the very high a* values in G1100 and Gg1100.

3.2.2.2. Radiography. The bricks with added household glass fired at higher temperatures have the highest densities. Fig. 7 shows brick cubes with two types of images, grey scale (original) and green–red variation, the latter highlighting the denser areas of the samples. The contrast makes it easier to observe the density difference between the bricks. The highest density is reached at the edges and decreases as we move inwards towards the core, as firing takes effect from the outside-in.

Jun samples made with added glass and fired at 950 °C and 1100 °C (Jg950 and Jg1100) show similar contrast intensity, which suggests that they have similar densities. However, Guadix samples with glass fired at 1100 °C are quite similar to Jun samples with glass fired at 800 °C. In addition, there is hardly any difference between the samples from Guadix fired at 800 and 950 °C. Radiography images suggest that, as firing temperature increases, a more or less (depending on the composition of bricks) vitreous phase develops, which increases the compactness [67].

3.2.3. Assessment of mechanical properties

3.2.3.1. Leeb hardness (LH) test. The hardness test results coincide with those of radiography (Fig. 7). Fig. 8 shows that the highest hardness values are observed on the surfaces and that they decrease towards the inside of the brick. This hardness is associated with higher density, i.e. the greater compactness of the bricks in these areas.

The bricks with added glass fired at 800 °C show similar hardness values (average values Jg800, 258 and Gg800, 267, respectively). This suggests that at 800 °C the glass is not yet acting as a flux agent and is not vitrifying the samples. Higher hardness values were obtained at 950 °C, especially in the bricks with added glass (average values of 304 in Jun and 272 in Guadix). The samples with the highest hardness values are those with added glass fired at 1100 °C (Jg1100 and Gg1100 with 449 and 393, respectively) (Fig. 8).

In the bricks made with clay from Guadix, the difference in hardness between the surface and the core increases by approximately 10 % when household glass is added, regardless of the firing temperature. This is not so evident in the bricks from Jun for which a similar percentage difference between surface and core hardness to that of the Guadix bricks can only be observed at 1100 °C. This different behaviour of Jun bricks may be due to the fact that more energy is consumed during the formation of Ca-(Mg-) silicate phases [57].

3.2.3.2. Ultrasonic pulse velocity (UPV). Table 3 shows the UPV values measured in the bricks with or without added glass. The preferential orientation of the phyllosilicates and other planar grains during the preparation of the raw material was perpendicular to the pressure that was exerted on the clayey earth when it was placed in the moulds. The P waves move more slowly perpendicular to these grains. The UPV of the

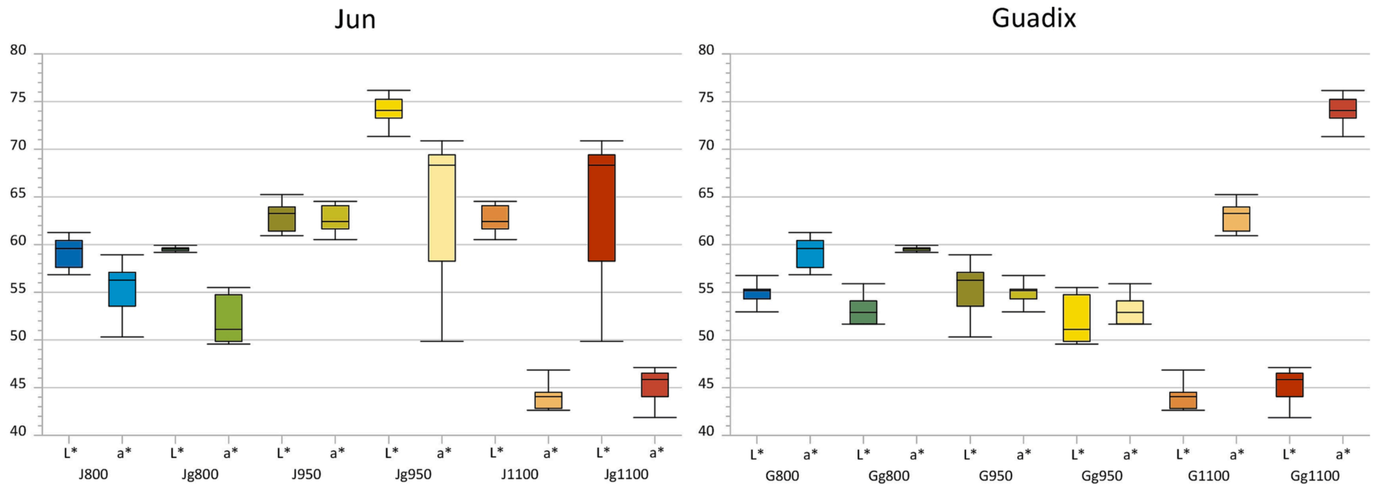

Fig. 6. Volume chart showing the lightness (L*) and a* values for bricks made with or without glass and fired at 800, 950 and 1100 °C.

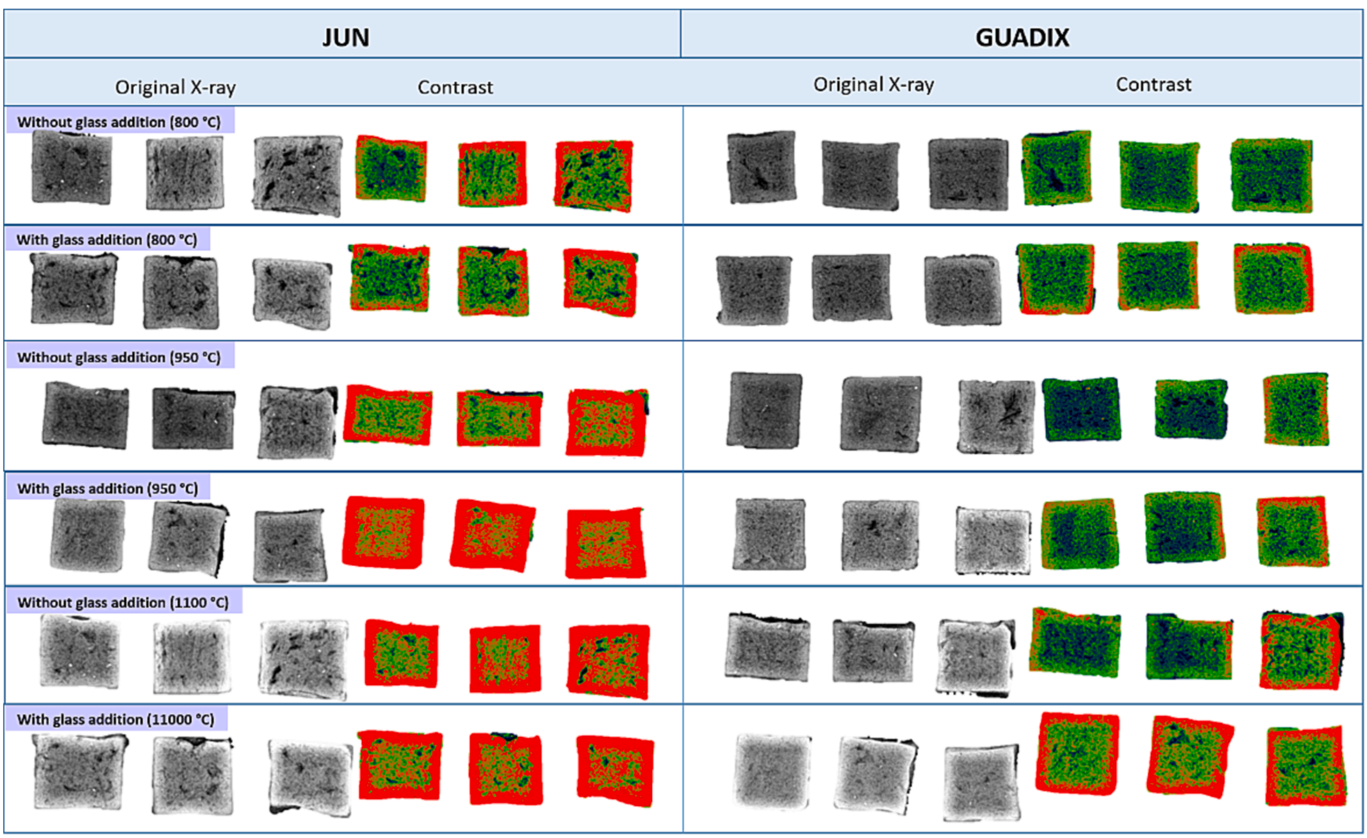

Fig. 7. X-rays of the bricks made with clay from Jun and Guadix with or without added glass and fired at 800, 950 and 1100 °C.

brick samples with added glass ranges between 1368 (Gg800) and 4625 m/s (Jg1100) (Table 3). A tendency towards lower velocity values was observed in the samples with no added glass, and the lowest was measured in sample G800 (Table 3, 1260 m/s). For bricks to be considered durable, the UPV value should be at least 1000 m/s [68]. This means that all the studied bricks studied here can be defined as durable. UPV values increase not only with the addition of glass but also in line with increases in the firing temperature.

3.2.3.3. Compressive strength (CS). The bricks made with clay from Jun, with or without added glass, showed higher compressive strength than those from Guadix (Table 3). In mineralogical terms, Changizi and Haddad [69] found that the compressive strength of bricks increases with the amount of quartz in the mix. However, if one looks at the mineralogy of the bricks from Jun and Guadix, the opposite applies: the bricks from Guadix are richer in quartz than those from Jun. In this case, the previous analyses show that the increase in compressive strength is related to the higher levels of vitrification produced by the addition of household glass [14]. In fact, the addition of glass always increases the strength of the bricks (Table 3). This increase is related to the textural and microstructural changes that take place in the bricks. As mentioned earlier, the glass acts as a flux agent bonding the particles together and reducing the porosity. The highest values were found for bricks fired at 1100 °C, due to their high level of vitrification. The sample with the

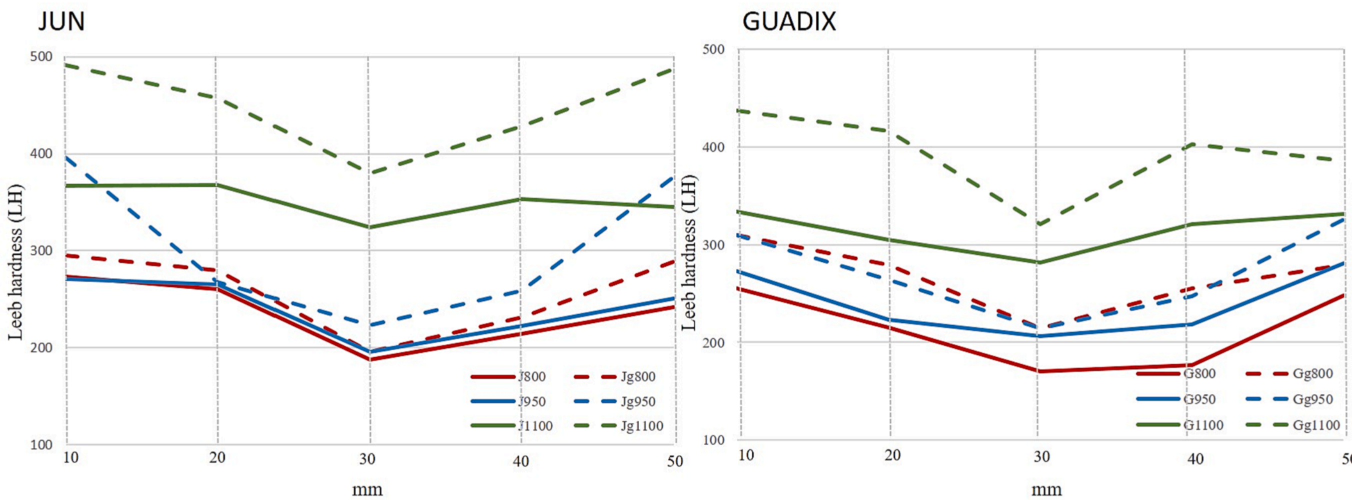

Fig. 8. Hardness (in LH) of bricks made with raw materials from Jun and Guadix with or without added glass and fired at 800, 950 and 1100 °C.

Table 3
Summary of average values ($\bar{x}$) for LH, UPV (m/s) and CS (Rc, MPa) and standard deviation (σ) values for handmade bricks made with raw materials from Jun and Guadix with or without added glass.

	LH		UPV (m/s)		CS (MPa)	
	$\bar{x}$	σ	$\bar{x}$V	Σ	$\bar{x}$	σ
J800	235	34.52	2667	87.71	19.18	5.09
J950	241	31.47	2650	143.73	20.23	8.15
J1100	351	18.12	2952	67.13	26.56	3.28
Jg800	258	42.97	2922	105.71	31.39	4.11
Jg950	304	76.70	2905	169.38	26.84	12.98
Jg1100	449	46.02	4625	250.51	72.58	5.07
G800	213	39.17	1260	59.83	6.43	0.34
G950	240	34.27	1853	191.39	12.34	3.15
G1100	315	21.45	2726	149.36	29.05	9.2
Gg800	267	35.67	1368	51.99	8.88	2.54
Gg950	272	45.86	2018	126.38	17.35	1.02
Gg1100	393	44.15	3346	200.92	35.28	15.03

highest compressive strength was Jg1100 (72.58 N/mm^2).

Several authors have found that the compressive strength of bricks is more closely linked to the porosity and the degree of vitrification than to the mineralogy of the raw material [39,67,68,69,70]. Tite and Maniatis [71] found that in bricks made with carbonate-rich clays, the structure formed at low temperatures (840–960 °C) remains almost unchanged until about 1080 °C. This is why the Jun samples (without added glass) fired at 800 and 950 °C show very similar CS values (Table 3 and Fig. 9). According to official specifications from the Spanish Ministry of Public Works (Pliego RL-88 [72]), all the samples, with the exception of G800, have enough compressive strength to be used for construction purposes.

In contrast to pore-forming additives, such as cigarette butts [73,74] wood sawdust [7] or grape stalks [8,16], the addition of glass improves the mechanical properties of the bricks.

4. Statistical analysis

The statistical analysis in this paper seeks to apply Tukey and Ducan's test (P < 5 %) to predict homogeneous subsets for the lightness (L*) and chromatic values (a*) taking into account the three firing temperatures for the same data population. The two types of clay (Jun and Guadix) and the addition or not of household glass were not considered because there are only two variables per type and this method requires at least three.

Three subsets (a, b and c) for L* and a* and two subsets (a and b) for b* were classified (Table 4). According to this method, there is a direct relationship between the lightness of the samples and the firing temperature, with higher temperature samples having higher lightness values. The average values for the bricks from Jun suggest that they follow this trend, while those from Guadix do not. This method also suggests that a* values increase in line with firing temperature. This was true for the Guadix bricks but not for those from Jun. This suggests that this method was unsuitable in that the properties of the bricks could not be determined solely on the basis of the firing temperature. The different combinations of clay with or without added glass might change the appearance of the bricks, a crucial issue in the restoration of architectural heritage.

The relationships between the mechanical properties determined by NDT, namely superficial hardness (Leeb), UPV and compressive strength (Table 4), were also explored. The study of the anisotropy enabled the correlation of the ultrasonic velocities with the microstructure (especially the pores/voids) of the samples in order to better understand the technical quality of the bricks, which is associated with the concept of anisotropic resistance. Homogeneous subsets were obtained according to Tukey and Ducan for the UPV, Leeb and compressive strength values taking into account the three firing temperatures for the same data population. These subsets were analysed and the data obtained confirmed the results of the NDT. It should be noted that for the UPV and compressive strength values, the values are divided into 3 subsets with an upward trend in line with temperature, while the Leeb values are only divided into 2 subsets. This makes it more difficult to compare the Leeb results with the results of other tests on physical–mechanical properties, such as UPV and compressive strength. Even so, this predictive method could be very useful for determining the mechanical properties.

5. Conclusions

In this paper, NDT were used to characterize bricks that were handmade with raw materials from two different sources, Jun and Guadix (Granada, Spain), fired at three different temperatures (800, 950 and 1100 °C), with or without added glass. The following conclusions were reached:

- The use of non-destructive techniques (NDT) revealed that the addition of glass increased the vitrification of the bricks and augmented their compressive strength.
- The colour of the bricks was mainly dependent on the type of raw material used, while the addition of household glass enhanced the lightness in the bricks made with clay from Jun and the a* parameter in the bricks made with clay from Guadix. Firing temperatures from

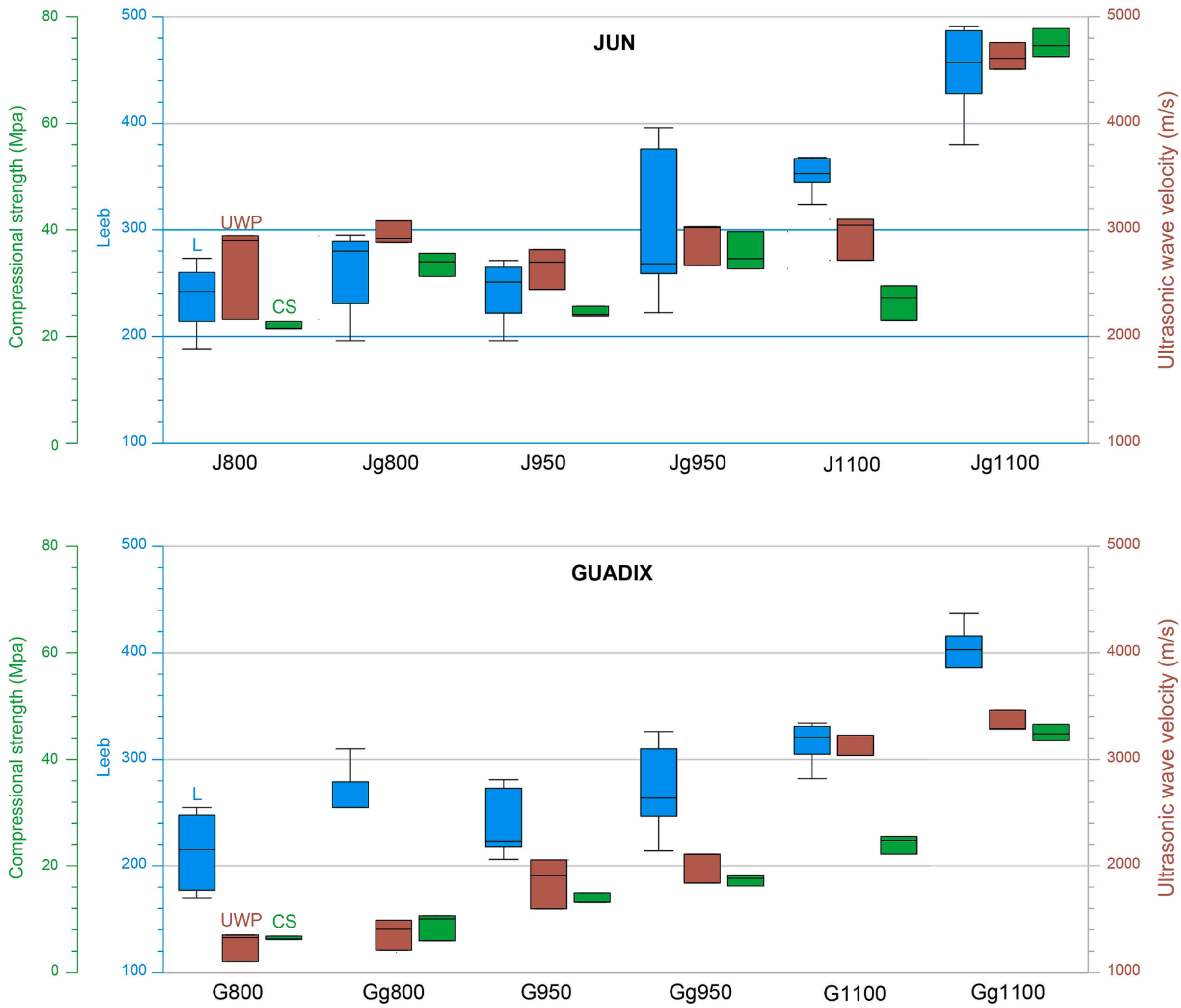

Fig. 9. Volume chart showing the LH, UPV and CS values for bricks made with or without added glass and fired at 800, 950 and 1100 °C.

Table 4
Classification of subsets (a, b and c) for aesthetic (L* a*and b*) and physical (UPV, LH and CS) properties according to the tests proposed by Tukey and by Ducan and the ANOVA method.

	L*	a*	b*	UPV	LH	CS
800 °C	53.75a	13.61a	18.98a	2054a	244a	17.58a
950 °C	56.63b	16.94b	26.53b	2356b	264a	20.85b
1100 °C	60.92c	19.02c	26.60b	3506c	377b	42.04c
ANOVA P values						
Raw material (RM)	0.000	0.000	0.000	0.000	0.036	0.000
Temperature (T)	0.000	0.000	0.000	0.000	0.000	0.000
Glass added (G)	0.023	0.000	0.000	0.000	0.000	0.000
RM × T	0.000	0.000	0.000	0.000	0.300	0.001
RM × G	0.000	0.000	0.000	0.000	0.770	0.000
G × T	0.019	0.000	0.000	0.000	0.153	0.000
RM × T × G	0.000	0.000	0.000	0.000	0.454	0.000

950 °C produced a significant aesthetic change in the bricks, which was especially visible in the samples with added glass, where glass bubbles can be seen "hatching" on the surface of the bricks.

- Radiography proved to be a very useful tool for observing the anisotropic distribution of density in the fired samples.
- In terms of mechanical properties, the bricks from Jun perform better than those from Guadix. However, the latter have better aesthetic properties, in the sense of more homogeneous colours, which can be a key factor when choosing a building material.
- The relationship between the aesthetic and the mechanical properties determined by NDT allows the results obtained from different analytical techniques to be compared, such as the relationship between density, as determined by x-rays, and surface hardness, as determined by Leeb. In this way, the density of the bricks can be compared with the hardness, both of which are greater on the surface and decrease towards the core, thus reducing the connectivity of the pores.
- According to the statistical predictions for the dependent variables of firing temperature using the tests proposed by Tukey and by Ducan,

regardless of whether they are fired with or without glass, the bricks made with clay from Jun tend to have higher mean values for all the variables than the bricks made with clay from Guadix. ANOVA analysis reveals that the clay from Jun performs better than the clay from Guadix. However, the bricks from Jun fired at 1100 °C and with added glass show the highest colour variations, which could make them less suitable for the restoration of architectural heritage, in which colour is a crucial factor.

CRediT authorship contribution statement

L. Crespo-López: Writing – review & editing, Writing – original draft, Visualization, Validation, Software, Resources, Methodology, Investigation, Formal analysis, Conceptualization. **D. Benavente:** Writing – review & editing, Validation, Supervision, Software, Investigation, Formal analysis, Data curation. **S. Morales-Ruano:** Supervision, Conceptualization. **M. Vázquez-Vílchez:** Supervision, Conceptualization. **G. Cultrone:** Writing – review & editing, Visualization, Validation, Supervision, Resources, Project administration, Methodology, Investigation, Funding acquisition, Formal analysis, Data curation, Conceptualization.

Declaration of Competing Interest

The authors declare that they have no known competing financial interests or personal relationships that could have appeared to influence the work reported in this paper.

Data availability

Data will be made available on request.

Acknowledgements

This study was funded by Junta de Andalucía Research Group RNM179 and by Research Project B.RNM.188.UGR20 of the Regional Ministry of University, Research and Innovation of the Junta de Andalucía and FEDER, *A way of making Europe*. We thank Cerámica Castillo Siles for providing the raw materials used to prepare the bricks and Nigel Walkington for his assistance in revising the English text of the manuscript. We also thank to the Clínica Veterinaria "Plaza de Toros" (https://cvpt.es/) who provided the radiological apparatus and helped to determine the appropriate working conditions.

Funding for open access charge

Universidad de Granada / CBUA.

References

[1] L. Zhang, Production of bricks from waste materials–a review, Constr. Build. Mater. 47 (2013) 643–655, https://doi.org/10.1016/j.conbuildmat.2013.05.043.
[2] S. Mukherjee, Environmental degradations during clay mining and beneficiation, in: The science of clays, Springer, Dordrecht, 2013, pp. 264–279, https://doi.org/10.1007/978-94-007-6683-9_18.
[3] A. Al-Fakih, B.S. Mohammed, M.S. Liew, E. Nikbakht, Incorporation of waste materials in the manufacture of masonry bricks: An update review, J. Build. Eng 21 (2019) 37–54, https://doi.org/10.1016/j.jobe.2018.09.023.
[4] A. Soni, P.K. Das, A.W. Hashmi, M. Yusuf, H. Kamyab, S. Chelliapan, Challenges and opportunities of utilizing municipal solid waste as alternative building materials for sustainable development goals: A review, Sustain. Chem. Pharm. 27 (2022), 100706, https://doi.org/10.1016/j.scp.2022.100706.
[5] S. Preethi, R. Prasannadevi, K. Preethi, S.R. Prasad, T.R. Banuchander, Reuse of plastic bottles in construction of buildings, Ratio 1 (10) (2019).
[6] K.G. Santhosh, S.M. Subhani, A. Bahurudeen, Sustainable reuse of palm oil fuel ash in concrete, alkali-activated binders, soil stabilisation, bricks and adsorbent: A waste to wealth approach, Ind. Crop. Prod. 183 (2022), 114954, https://doi.org/10.1016/j.indcrop.2022.114954.
[7] G. Cultrone, I. Aurrekoetxea, C. Casado, A. Arizzi, Sawdust recycling in the production of lightweight bricks: How the amount of additive and the firing temperature influence the physical properties of the bricks, Constr. Build. Mater. 235 (2020), 117436, https://doi.org/10.1016/j.conbuildmat.2019.117436.
[8] C. Coletti, E. Bragié, M.C. Dalconi, C. Mazzoli, A. Hein, L. Maritan, A new brick-type using grape stalks waste from wine production as pore-agent, Open Ceramics 14 (2023), 100365, https://doi.org/10.1016/j.oceram.2023.100365.
[9] M. López Gómez, G. Cultrone, The use of expanded polystyrene and olive stones in the manufacture of lightweight bricks: evaluation of their properties and durability, Materials 16 (4) (2023) 1330, https://doi.org/10.3390/ma16041330.
[10] A. Karslioğlu, E. Balaban, M.İ. Onur, Insulation properties of bricks with waste rubber and plastic: a review, J. Nat. 1 (2021) 20–27, https://doi.org/10.36937/janset2021.001.004.
[11] D. Eliche-Quesada, C. Martínez-García, M.L. Martínez-Cartas, M.T. Cotes-Palomino, L. Pérez-Villarejo, N. Cruz-Pérez, F.A. Corpas-Iglesias, The use of different forms of waste in the manufacture of ceramic bricks, Appl. Clay Sci. 52 (3) (2011) 270–276, https://doi.org/10.1016/j.clay.2011.03.003.
[12] F.V. Simão, H. Chambart, L. Vandemeulebroeke, P. Nielsen, L.R. Adrianto, S. Pfister, V. Cappuyns, Mine waste as a sustainable resource for facing bricks, J. Clean. Prod. 368 (2022), 133118, https://doi.org/10.1016/j.jclepro.2022.133118.
[13] G. D'Angelo, M. Fumo, M. Merino, I. Capasso, A. Campanile, F. Iucolano, D. Caputo, B. Liguori, Crushed bricks: demolition waste as a sustainable raw material for geopolymers, Sustainability 13 (2021) 7572, https://doi.org/10.3390/su13147572.
[14] L. Crespo-López, G. Cultrone, Improvement in the petrophysical properties of solid bricks by adding household glass waste, J. Build. Eng 59 (2022), 105039, https://doi.org/10.1016/j.jobe.2022.105039.
[15] G. Cultrone, The use of Mount Etna volcanic ash in the production of bricks with good physical-mechanical performance: converting a problematic waste product into a resource for the construction industry, Ceram. Int. 48 (4) (2022) 5724–5736, https://doi.org/10.1016/j.ceramint.2021.11.119.
[16] L. Crespo-López, A. Martínez-Ramirez, E. Sebastián, G. Cultrone, Pomace from the wine industry as an additive in the production of traditional sustainable lightweight eco-bricks, Appl. Clay Sci. 243 (2023), 107084, https://doi.org/10.1016/j.clay.2023.107084.
[17] T. Teschemacher, P. Wilson, R. Wüchner, K.U. Bletzinger, Macroscopic characterization of modern masonry, Struct. Eng. 268 (2022), 114630, https://doi.org/10.1016/j.engstruct.2022.114630.
[18] M. Rosa, F. Lorenzoni, R. Deiana, S. Taffarel, C. Modena, 2019. Non-destructive investigations for structural qualification of the Sarno Baths, Pompeii. J Cult Herit. https://doi.org/10.1016/j.culher.2019.04.015.
[19] E. Mesquita, R. Martini, A. Alves, P. Antunes, H. Varum, Non-destructive characterization of ancient clay brick walls by indirect ultrasonic measurements, J. Build. Eng. 19 (January) (2018) 172–180, https://doi.org/10.1016/j.jobe.2018.05.011.
[20] L.F. Ramos, L. Marques, P.B. Lourenço, G. De Roeck, A. Campos-Costa, J. Roque, Monitoring historical masonry structures with operational modal analysis: two case studies, Mech. Syst. Sig. Process. 24 (5) (2010) 1291–1305, https://doi.org/10.1016/j.ymssp.2010.01.011.
[21] E. Mesquita, P. Antunes, F. Coelho, P. Andre, Global overview on advances in structural health monitoring platforms, J. Civ. Struct. Health Monit. 6 (3) (2016) 461–475, https://doi.org/10.1007/s13349-016-0184-5.
[22] L.F. Miranda, J. Rio, G.J. Miranda, A. Costa, Sonic impact method—a new technique for characterization of stone masonry walls, Constr. Build. Mater. 36 (2012) 27–35, https://doi.org/10.1016/j.conbuildmat.2012.04.018.
[23] C. Viseras, Estratigrafía y sedimentología del relleno aluvial de la Cuenca de Guadix (Cordilleras Béticas), Universidad de Granada, 1991, p. 327. Ph.D. Thesis.
[24] J.M. García-Aguilar, J.M. Martín, Late Neogene to recent continental history and evolution of the Guadix-Baza Basin (SE Spain), Rev. Soc. Geol. 13 (2000) 65–77.
[25] A. Granados, O. Oms, P. Anadón, J. Ibanez-Insa, A. Kaakinen, J.M. Jiménez-Arenas, Geochemical and sedimentary constraints on the formation of the Venta Micena Early Pleistocene site (Guadix-Baza basin, Spain), Sci. Rep. 11 (1) (2021) 1–13, https://doi.org/10.1038/s41598-021-01711-7.
[26] A. García-Alix, R. Minwer-Barakat, J.M. Martín, E. Martín-Suárez, M. Freudenthal, Biostratigraphy and sedimentary evolution of late Miocene and Pliocene continental deposits of the Granada Basin (southern Spain), Lethaia 41 (2008) 431–446, https://doi.org/10.1111/j.1502-3931.2008.00097.x.
[27] V. Loryuenyong, T. Panyachai, K. Kaewsimork, C. Siritai, Effects of recycled glass substitution on the physical and mechanical properties of clay bricks, J. Waste Manag. 29 (10) (2009) 2717–2721, https://doi.org/10.1016/j.wasman.2009.05.015.
[28] Z. Zhang, Y.C. Wong, M. Sofi, P. Mendis, Incorporation of glass and plastic waste into alkali-activated mill residue bricks, Sustainability 14 (24) (2022) 16533, https://doi.org/10.3390/su142416533.
[29] L. Mao, H. Zhou, M. Peng, L. Hu, W. Zhang, Effects of waste glass particle size on improving the property and environmental safety of fired brick containing electroplating sludge, Constr. Build. Mater. 257 (2020), 119583, https://doi.org/10.1016/j.conbuildmat.2020.119583.
[30] R.T. Laird, M. Worcester, The inhibiting of lime blowing, Br. Ceram. Trans. 55 (1956) 545–563.
[31] D.M. Moore, R.C. Reynolds Jr., X-ray Diffraction and the Identification and Analysis of Clay Minerals, Oxford University Press (OUP), 1989.
[32] UNE-EN 15886, Métodos de ensayo, Medición del color de superficies, AENOR, Madrid, 2011.
[33] M. Gomez-Heras, D. Benavente, C. Pla, J. Martinez-Martinez, R. Fort, V. Brotons, Ultrasonic pulse velocity as a way of improving uniaxial compressive strength

estimations from Leeb hardness measurements, Constr. Build. Mater. 261 (2020), 119996, https://doi.org/10.1016/j.conbuildmat.2020.119996.
[34] ASTM D2845, Standard test method for laboratory determination of pulse velocities and ultrasonic elastic constants of rock, J. ASTM Int., West Conshohocken, PA, USA, 2000.
[35] UNE-EN 772-1:2000. Métodos de ensayo de piezas para fábrica de albañilería. Parte 1: Determinación de la resistencia a compresión. AENOR, Madrid.
[36] M.C. Jollands, M. Blanchard, E. Balan, Structure and theoretical infrared spectra of OH defects in quartz, Eur. J. Mineral. 32 (2020) 311–323, https://doi.org/10.5194/ejm-32-311-2020.
[37] H.W. Nesbitt, G.M. Bancroft, G.S. Henderson, Temperature dependence of Raman shifts and line widths for Q^0 and Q^2 crystals of silicates, phosphates, and sulphates, Am. Mineral. 103 (2018) 966–976, https://doi.org/10.2138/am-2018-6314.
[38] P. Saravanapavan, L.L. Hench, Mesoporous calcium silicate glasses. I. Synthesis, J. Non-Cryst. Solids 318 (1–2) (2003) 1–13, https://doi.org/10.1016/S0022-3093.
[39] T.K. Dan, S. Raman, Physico-chemical analysis of a raw brick clays of Bhopal, Indian Ceramics (1986).
[40] A.E. Lavat, M.C. Grasselli, J.E. Tasca, Phase changes of ceramic whiteware slip-casting bodies studied by XRD and FTIR, Ceram. Int. 33 (6) (2007) 1111–1117, https://doi.org/10.1016/j.ceramint.2006.03.016.
[41] H. Liu, Y. Wei, P. Li, Y. Zhang, Y. Sun, Catalytic synthesis of nanosized hematite particles in solution, Mater. Chem. Phys. 102 (1) (2007) 1–6, https://doi.org/10.1016/j.matchemphys.2006.10.001.
[42] E. Darezereshki, Synthesis of maghemite (γ-Fe2O3) nanoparticles by wet chemical method at room temperature, Mater. Lett. 64 (13) (2010) 1471–1472, https://doi.org/10.1016/j.matlet.2010.03.064.
[43] S.S. Amritphale, N. Chandra, R. Kumar, Sintering behaviour of pyrophyllite mineral: effect of some alkali and alkaline-earth metal carbonates, J. Mater. Sci. 27 (17) (1992) 4797–4804, https://doi.org/10.1007/BF01166022.
[44] T. Shimanouchi, Tables of Molecular Vibrational Frequencies, US Government Printing Office, 1973.
[45] T.K. Mukhopadhyay, S. Ghatak, H.S. Maiti, Pyrophyllite as raw material for ceramic applications in the perspective of its pyro-chemical properties, Ceram. Int. 36 (3) (2010) 909–916, https://doi.org/10.1016/j.ceramint.2009.10.026.
[46] J.L. Post, L. Borer, Physical properties of selected illites, beidellites and mixed-layer illite–beidellites from southwestern Idaho, and their infrared spectra, Appl. Clay Sci. 22 (3) (2002) 77–91, https://doi.org/10.1016/S0169-1317(02)00129-1.
[47] A. Elimbi, H.K. Tchakoute, D. Njopwouo, Effects of calcination temperature of kaolinite clays on the properties of geopolymer cements, Construc. Build. Mater. 25 (6) (2011) 2805–2812, https://doi.org/10.1016/j.conbuildmat.2010.12.055.
[48] K.H. Hellwege, W. Lesch, M. Plihal, G. Schaack, Zwei-phononen-absorptionsspektren und dispersion der schwingungszweige in kristallen der kalkspatstruktur, Zeitschrift Für Physik A Hadrons and Nuclei 232 (1) (1970) 61–86, https://doi.org/10.1007/BF01394946.
[49] R.N. Panda, M.F. Hsieh, R.J. Chung, T.S. Chin, FTIR, XRD, SEM and solid state NMR investigations of carbonate-containing hydroxyapatite nano-particles synthesized by hydroxide-gel technique, J. Phys. Chem. Solid 64 (2) (2003) 193–199, https://doi.org/10.1016/S0022-3697(02)00257-3.
[50] H.K. Choudhary, A.V. Anupama, R. Kumar, M.E. Panzi, S. Matteppanavar, B. N. Sherikar, B. Sahoo, Observation of phase transformations in cement during hydration, Constr. Build. Mater. 101 (2015) 122–129, https://doi.org/10.1016/j.conbuildmat.2015.10.027.
[51] E. Balan, J. Aufort, G.D. Saldi, C. Brouder, M. Lazzeri, Line-broadening and anharmonic effects in the attenuated total reflectance infrared spectra of calcite, Eur. J. Mineral. 31 (2019) 73–81, https://doi.org/10.1127/ejm/2018/0030-2802.
[52] R.V. Barde, K.R. Nemade, S.A. Waghuley, AC conductivity and dielectric relaxation in V_2O_5–P_2O_5–B_2O_3 glasses, J. Asian Ceram. Soc. 3 (1) (2015) 116–122, https://doi.org/10.1016/j.jascer.2014.11.006.
[53] D.P. Mukherjee, S.K. Das, Effects of nano silica on synthesis and properties of glass ceramics in SiO_2–Al_2O_3–CaO–CaF_2 glass system: A comparison, J. Non Cryst. Solids 368 (2013) 98–104, https://doi.org/10.1016/j.jnoncrysol.2013.03.012.
[54] S.A. MacDonald, C.R. Schardt, D.J. Masiello, J.H. Simmons, Dispersion analysis of FTIR reflection measurements in silicate glasses, J. Non Cryst. Solids 275 (1–2) (2000) 72–82, https://doi.org/10.1016/S0022-3093(00)00121-6.
[55] L.A. Zellmer, W.B. White, Characterization of hydrated surface layers on nuclear waste glasses by infrared reflectance spectroscopy, MRS Online Proceedings Library (OPL) 44 (1984), https://doi.org/10.1557/PROC-44-73.
[56] R.D. Husung, R.H. Doremus, The infrared transmission spectra of four silicate glasses before and after exposure to water, J. Mater. Res. 5 (10) (1990) 2209–2217, https://doi.org/10.1557/JMR.1990.2209.
[57] G. Cultrone, C. Rodriguez-Navarro, E. Sebastian, O. Cazalla, M.J. De La Torre, Carbonate and silicate phase reactions during ceramic firing, Eur. J. Mineral. 13 (3) (2001) 621–634, https://doi.org/10.1127/0935-1221/2001/0013-0621.
[58] L.N. Warr, Recommended abbreviations for the names of clay minerals and associated phases, Clay Miner. 55 (3) (2020) 261–264, https://doi.org/10.1180/clm.2020.30.
[59] J. Parras, C. Sánchez-Jimeńez, M. Rodas, F.J. Luque, Ceramic applications of Middle Ordovician shales from central Spain, Appl. Clay Sci. 11 (1) (1996) 25–41, https://doi.org/10.1016/0169-1317(96)00003-8.
[60] C. Rathossi, Y. Pontikes, Effect of firing temperature and atmosphere on ceramics made of NW Peloponnese clay sediments. Part I: Reaction paths, crystalline phases, microstructure and colour, J. Eur. Ceram. Soc. 30 (9) (2010) 1841–1851, https://doi.org/10.1016/j.jeurceramsoc.2010.02.002.
[61] J. Capel, F. Huertas, J. Linares, High temperature reactions and use of bronze age pottery from La Mancha, central Spain, Mineral. Petrogr. Acta 29 (1985) 563–575.
[62] G. Cultrone, F.J.C. Rosua, Growth of metastable phases during brick firing: Mineralogical and microtextural changes induced by the composition of the raw material and the presence of additives, Appl. Clay Sci. 185 (2020), 105419, https://doi.org/10.1016/j.clay.2019.105419.
[63] A.C.P. Galvao, A.C.M. Farias, J.U.L. Mendes, Characterization of waste of soda-lime glass generated from lapping process to reuse as filler in composite materials as thermal insulation, Ceramica 61 (359) (2015) 367–373, https://doi.org/10.1590/0366-69132015613591987.
[64] J.D. Bautista-Marín, A. Esguerra-Arce, J. Esguerra-Arce, Use of an industrial solid waste as a pigment in clay bricks and its effects on the mechanical properties, Constr. Build. Mater. 306 (2021), 124848, https://doi.org/10.1016/j.conbuildmat.2021.124848.
[65] Y. Maniatis, A. Simopoulos, A. Kostikas, V. Perdikatsis, Effect of reducing atmosphere on minerals and iron oxides developed in fired clays: the role of Ca, J. Am. Ceram. Soc. 66 (11) (1983) 773–781, https://doi.org/10.1111/j.1151-2916.1983.tb10561.x.
[66] A. De Bonis, G. Cultrone, C. Grifa, A. Langella, A.P. Leone, M. Mercurio, V. Morra, Different shades of red: The complexity of mineralogical and physico-chemical factors influencing the colour of ceramics, Ceram. Int. 43 (11) (2017) 8065–8074, https://doi.org/10.1016/j.ceramint.2017.03.127.
[67] G. Cultrone, E. Sebastián, K. Elert, M.J. De la Torre, O. Cazalla, C. Rodriguez-Navarro, Influence of mineralogy and firing temperature on the porosity of bricks, J. Eur. Ceram. Soc. 24 (3) (2004) 547–564, https://doi.org/10.1016/S0955-2219(03)00249-8.
[68] F. Hei, Q. Liu, G. Zhao, J. Ou, F. Xu, Preparation and characteristics of the fired bricks produced from polyaluminum chloride slag and glass powder, Appl. Sci. 13 (3) (2023) 1989, https://doi.org/10.3390/app13031989.
[69] F. Changizi, A. Haddad, Strength properties of soft clay treated with mixture of nano-SiO2 and recycled polyester fiber, J. Rock Mech. Geotech. Eng. 7 (4) (2015) 367–378, https://doi.org/10.1016/j.jrmge.2015.03.013.
[70] K. Elert, G. Cultrone, C.R. Navarro, E.S. Pardo, Durability of bricks used in the conservation of historic buildings—influence of composition and microstructure, J. Cult. Herit. 4 (2) (2003) 91–99, https://doi.org/10.1016/S1296-2074(03)00020-7.
[71] M.S. Tite, Y. Maniatis, Scanning Electron Microscope of Fired Calcareous Clays.Br. Ceram. Trans., No. 74, 1975, 19-22.
[72] Pliego RL-88, Pliego General de Condiciones para la Recepción de Ladrillos Cerámicos en las Obras de Construcción, Ministerio de Obras Públicas, Transportes y Medio Ambiente, Spain, 1988.
[73] A.A. Kadir, A. Mohajerani, Effect of heating rate on gas emissions and properties of fired clay bricks and fired clay bricks incorporated with cigarette butts, Appl. Clay Sci. 104 (2015) 269–276, https://doi.org/10.1016/j.clay.2014.12.005.
[74] A. Mohajerani, A.A. Kadir, L. Larobina, A practical proposal for solving the world's cigarette butt problem: recycling in fired clay bricks, J. Waste Manag. 52 (2016) 228–244, https://doi.org/10.1016/j.wasman.2016.03.012.